analytical chemistry

Article

Cite This: Anal. Chem. 2018, 90, 14287−14293

pubs.acs.org/ac

Dynamic Imaging of Small Molecule Induced Protein−Protein Interactions in Living Cells with a Fluorophore Phase Transition Based Approach

Chan-I Chung,[†,‡] Qiang Zhang,[†,‡] and Xiaokun Shu*[,†,‡]

[†]Department of Pharmaceutical Chemistry, University of California—San Francisco, San Francisco, California 94158-9001, United States

[‡]Cardiovascular Research Institute, University of California—San Francisco, San Francisco, California94158-9001, United States

Supporting Information

ABSTRACT: Protein−protein interactions (PPIs) mediate signal transduction in cells. Small molecules that regulate PPIs are important tools for biology and biomedicine. Dynamic imaging of small molecule induced PPIs characterizes and verifies these molecules in living cells. It is thus important to develop cellular assays for dynamic visualization of small molecule induced protein−protein association and dissociation in living cells. Here we have applied a fluorophore phase transition based principle and designed a PPI assay named SPPIER (separation of phases-based protein interaction reporter). SPPIER utilizes the green fluorescent protein (GFP) and is thus genetically encoded. Upon small molecule induced PPI, SPPIER rapidly forms highly fluorescent GFP droplets in living cells. SPPIER detects immunomodulatory drug (IMiD) induced PPI between cereblon and the transcription factor Ikaros. It also detects IMiD analogue (e.g., CC-885) induced PPI between cereblon and GSPT1. Furthermore, SPPIER can visualize bifunctional molecules (e.g. PROTAC)-induced PPI between an E3 ubiquitin ligase and a target protein. Lastly, SPPIER can be modified to image small molecule induced protein−protein dissociation, such as nutlin-induced dissociation between HDM2 and p53. The intense brightness and rapid kinetics of SPPIER enable robust and dynamic visualization of PPIs in living cells.

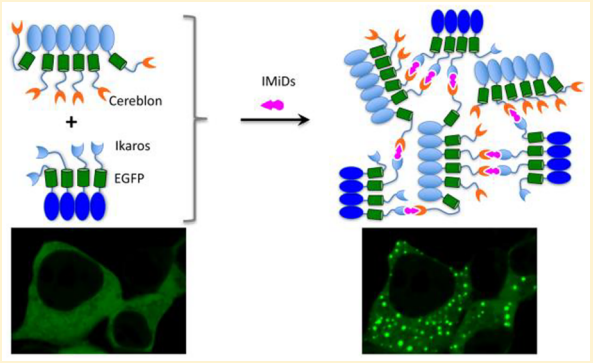

INTRODUCTION

Small molecules that modulate protein−protein interactions (PPIs) are important tools for biological investigation and therapeutic intervention.[1] For example, immunomodulatory drugs (IMiDs) bind to the E3 ligase cereblon and induce interaction between cereblon and the transcription factor Ikaros, leading to ubiquitination and degradation of the transcription factor.[2] The cereblon-based degradation of Ikaros accounts for the clinical efficacy of IMiDs such as lenalidomide against multiple myeloma.[3−5] Another example is nutlin, which binds to the E3 ligase HDM2 and disrupts its interaction with the transcription factor p53, resulting in stabilization of p53, leading to cell cycle arrest and apoptosis of cancer cells.[6] It is thus important to develop cellular assays for imaging small molecule induced protein−protein association as well as dissociation in living cells.

An ideal assay to detect small molecule induced PPI should have large fluorescence change, high brightness, and rapid and reversible kinetics and be applicable to live cells so that the PPI is detected in the context of living cells. Here we decided to apply a GFP phase transition based principle and design a cellular assay (named SPPIER for separation of phases-based protein interaction reporter) for detecting small molecule induced PPI. GFP has been widely used as a fluorescent tag in live cells and has revolutionized molecular and cell biology, because its fluorescence is genetically encoded and requires no cofactors except molecular oxygen.[7,8]

SPPIER is an addition to many other genetically encoded PPI detection methods, including bimolecular fluorescence complementation (BiFC),[9,10] fluorescence resonance energy transfer (FRET),[11] and dimerization-dependent fluorescent proteins (ddFP).[12,13] All of these assays have their own advantages and limitations. For example, while the fluorophore phase transition based assay achieves high brightness and large fluorescence change, it lacks spatial resolution and the introduced oligomeric tags might perturb protein function. On the other hand, BiFC, FRET, and ddFP achieve better spatial resolution in detecting PPIs but their signal over noise is smaller than that of SPPIER. On the basis of their advantages and limitations, these assays can fulfill different needs or purposes in detecting various PPIs.

Received: August 2, 2018
Accepted: November 15, 2018
Published: November 15, 2018

DOI: 10.1021/acs.analchem.8b03476
Anal. Chem. 2018, 90, 14287−14293

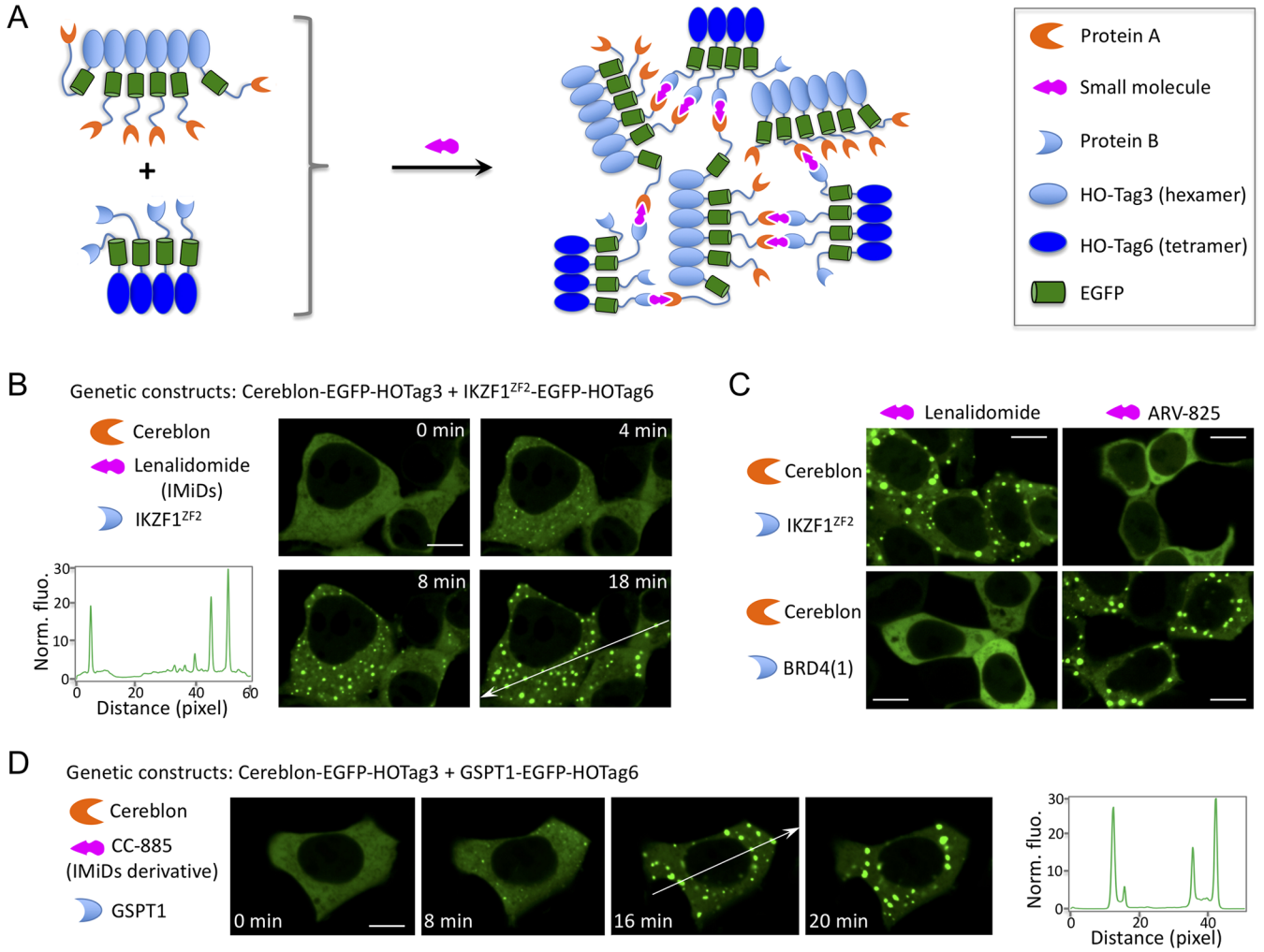

Figure 1. Fluorophore phase separation-based assay for imaging IMiD and its derivative-induced protein−protein interactions in living cells. (A). Schematic diagram showing the design of the cellular assay. (B). Fluorescence images showing detection of IMiD (lenalidomide)-induced interaction between the E3 ligase cereblon and the transcription factor Ikaros. A fluorescence histogram of the line across the cells is shown on the right. HEK293 cells transiently expressed CRBN-EGFP-HOTag3 and IKZF1^{ZF2}-EGFP-HOTag6. Lenalidomide (1 μM) was added to the cells. (C). Specificity of SPPIER. HEK293 cells transiently expressed CRBN-EGFP-HOTag3 and BRD4(1)-EGFP-HOTag6 or CRBN-EGFP-HOTag3 and IKZF1^{ZF2}-EGFP-HOTag6. Lenalidomide (1 μM) or ARV-825 (1 μM) was added to the cells. (D). Fluorescence images showing detection of an IMiD derivative, CC-885, induced interaction between the E3 ligase cereblon and GSPT1. A fluorescence histogram of the line across the cells is shown on the right. HEK293 cells transiently expressed CRBN-EGFP-HOTag3 and GSPT1-EGFP-HOTag6. CC-885 (1 μM) was added to the cells. Scale bar: 10 μm.

For example, many of the genetically encoded PPI assays such as FRET have been used in high content screening (HCS),[14] but their application has been limited in HCS due to small signal over noise. On the other hand, our fluorophore phase transition based assay will be advantageous for HCS because of its large fluorescence change, high brightness, and easily recognizable signal pattern.

EXPERIMENTAL SECTION

Plasmid Construction. All plasmid constructs were created by standard molecular biology techniques and confirmed by exhaustively sequencing the cloned fragments. To create E3 ubiqutin ligase (e.g., CRBN, VHL)-EGFP-HOTag3 fusions, the target protein was first cloned into pcDNA3 containing EGFP. HOTag3 was then cloned into the pcDNA3 E3 ligase-EGFP construct, resulting in pcDNA3 E3 ligase-EGFP-HOTag3. Similar procedures were carried out to produce pcDNA3 target protein (e.g., BRD4(1), IKZF1^{ZF2})-EGFP-HOTag6. To create the inducible SPPIER, FKBP12-EGFP-HOTag3 and Frb-p53^{TAD}-HOTag6 were created by a similar procedure; Hdm2^{p53BD}-IFP2 fusion was created by linking the DNA sequence of Hdm2^{p53BD} and IFP2, which was subsequently cloned into a pcDNA3 vector.

Cell Culture. The HEK293*T*/17 cells were passaged in Dulbecco's modified Eagle medium (DMEM) supplemented with 10% fetal bovine serum (FBS), nonessential amino acids, penicillin (100 units/mL), and streptomycin (100 μg/mL). All culture supplies were obtained from the UCSF Cell Culture Facility.

Live Cell Imaging. HEK293*T*/17 cells were transiently transfected with the plasmid using calcium phosphate transfection reagent or lipofectamine. Cells were grown in 35 mm glass bottom microwell (14 mm) dishes (MatTek Corporation). Transfection was performed when cells were cultured to ~50% confluence. For each transfection, 4.3 μg of plasmid DNA was mixed with 71 μL of 1X Hanks' Balanced Salts buffer

DOI: 10.1021/acs.analchem.8b03476
Anal. Chem. 2018, 90, 14287−14293

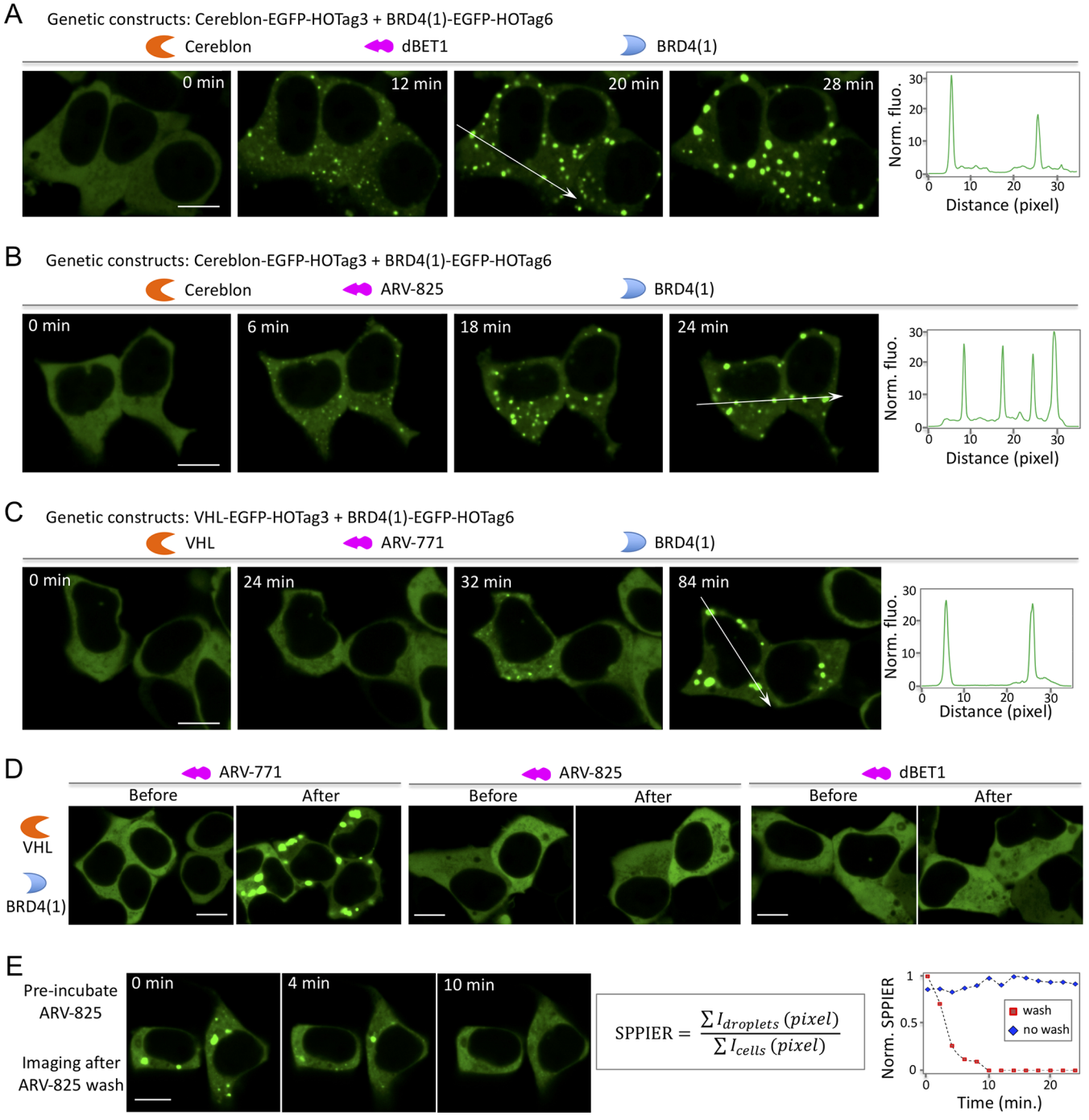

Figure 2. SPPIER detects bifunctional molecule induced protein−protein interaction in living cells. (A) Detection of dBET1 (5 μM)-induced interaction between the E3 ligase cereblon (CRBN) and BRD4(1). The fluorescence histogram of the line across the cells is shown on the right. HEK293 cells transiently expressed CRBN-EGFP-HOTag3 and BRD4(1)-EGFP-HOTag6. (B) Detection of a ARV-825 (0.1 μM)-induced interaction between the E3 ligase cereblon (CRBN) and BRD4(1). (C) Detection of ARV-771 (1 μM)-induced interaction between the E3 ligase VHL and BRD4. HEK293 cells transiently expressed VHL-EGFP-HOTag3 and BRD4(1)-EGFP-HOTag6. (D) Specificity of SPPIER. HEK293 cells transiently expressed VHL-EGFP-HOTag3 and BRD4(1)-EGFP-HOTag6. ARV-771 (1 μM), ARV-825 (1 μM), or 5 μM dBET1 (5 μM) was added to the cells. Images were taken before and (2 h) after addition of the bifunctional molecule. (E) SPPIER is reversible. Cells were preincubated with ARV-825. Scale bar: 10 μm.

(HBS) and 4.3 μL of 2.5 M $CaCl_2$. Cells were imaged 24 h after transient transfection. Time-lapse imaging was performed with the aid of an environmental control unit incubation chamber (InVivo Scientific), which was maintained at 37 °C and 5% CO_2. Fluorescence images were acquired with an exposure time of 50 ms for EGFP and 200 ms for IFP2. Chemical reagents, including IMiDs (lenalidomide) and derivatives (CC-885), rapamycin, nutlin-3a, and various bifunctional molecules (ARV-825, dBET1, ARV-771), were carefully added to the cells in the incubation chamber when the time-lapse imaging was started. Image acquisition was controlled by the NIS-Elements Ar Microscope Imaging Software (Nikon). Images were processed using NIS-Elements and ImageJ (NIH).

DOI: 10.1021/acs.analchem.8b03476
Anal. Chem. 2018, 90, 14287−14293

Image Analysis. For analysis of the SPPIER signal, images were processed in imageJ. The sum of droplet pixel fluorescence intensity and cell pixel intensity was scored using the Analyze Particle function in imageJ.

RESULTS AND DISCUSSION

Designing a Cellular Assay for Detecting Small Molecule Induced PPI. Our assay is based on a multivalent PPI-induced protein phase transition, which leads to the formation of highly concentrated protein droplets.[15,16] Here, to introduce multivalency, we utilized a de novo designed coiled coil as a homo-oligomeric tag (HO-Tag). To obtain fluorescence, we incorporated the enhanced GFP (EGFP) into the reporter because its use in living cells has been validated in many contexts. In particular, to design a PPI assay for detecting small molecule induced interaction between protein A and protein B, we genetically fused a short coiled coil-based HO-Tag3 (hexamer, 30 amino acid (aa)) to protein A and another coiled coil-based HO-Tag6 (tetramer, 33aa, Figure S1 in the Supporting Information)[17,18] to protein B (Figure 1A). Upon small molecule induced PPI between proteins A and B, each hexameric A-EGFP-HOTag3 protein recruits six B-EGFP-HOTag6 proteins. Then each tetrameric B-EGFP-HOTag6 protein recruits four A-EGFP-HOTag3 proteins, and so on. Eventually the HO-Tag-introduced multivalency and the protein A/B interactions lead to EGFP phase separation, forming highly fluorescent green EGFP droplets. We named this PPI assay SPPIER for separation of phases-based protein interaction reporter. SPPIER is similar to a previous assay named Fluoppi.[19] While Fluoppi uses tetrameric fluorescent proteins, SPPIER is not limited to oligomeric fluorescent proteins.

SPPIER Visualizes IMiD-Induced Interaction between Cereblon and Ikaros. IMiDs, such as lenalidomide, are small molecules that induce PPI between the E3 ubiquitin ligase cereblon and the transcription factor Ikaros.[3,20] To show whether SPPIER can detect IMiD-induced PPI, we genetically fused HO-Tag3 and EGFP to cereblon and HO-Tag6 to the zinc finger domain 2 (ZF2) of Ikaros ($IKZF1^{ZF2}$). Coexpression of CRBN-EGFP-HOTag3 and $IKZF1^{ZF2}$-EGFP-HOTag6 in the human embryonic kidney 293 (HEK293) cells revealed homogeneous fluorescence (Figure 1B). Addition of lenalidomide led to EGFP droplet formation within a few minutes (Video 1 in the Supporting Information), indicating that SPPIER can detect IMiD-induced PPI.

We next examined the specificity of SPPIER. While lenalidomide induces interaction between cereblon and Ikaros, another small molecule named ARV-825 induces interaction between cereblon and BRD4(1) (see below). First, we coexpressed CRBN-EGFP-HOTag3 and $IKZF1^{ZF2}$-EGFP-HOTag6 in the HEK293 cells. Addition of lenalidomide led to droplet formation (Figure 1C). In contrast, addition of ARV-825 did not result in any droplet formation. Next, we coexpressed CRBN-EGFP-HOTag3 and BRD4(1)-EGFP-HOTag6 in HEK293 cells. While lenalidomide did not induce any droplet formation, ARV-825 induced EGFP droplet formation. These data demonstrate that SPPIER achieves specificity in PPI detection.

SPPIER Visualizes IMiD Analogue Induced Interaction between Cereblon and GSPT1. Because of the successful applications of SPPIER in imaging of IMiD-induced PPIs, we next decided to examine if SPPIER can detect small molecules that are derived from IMiDs. Many analogues and derivatives of IMiDs have recently been designed and explored as drug leads against cancer. CC-885, one IMiD derivative, has been shown to induce interaction between CRBN and GSPT1.[21] To examine whether SPPIER can detect CC-885-induced PPI, we genetically fused HO-Tag6 to GSPT1 and coexpressed GSPT1-EGFP-HOTag6 and CRBN-EGFP-HOTag3 in HEK293 cells. Time-lapse imaging revealed that the coexpressed fusion proteins were homogeneously fluorescent (Figure 1D). Addition of CC-885 led to intensely bright and punctal green fluorescence (Video 2 in the Supporting Information). Thus, SPPIER also detects CC-885-induced PPI. The result suggests that SPPIER can be a powerful assay to screen IMiD analogues and derivatives targeting specific proteins in live cells.

SPPIER Visualizes Bifunctional Molecule Induced PPI. To further demonstrate SPPIER, we decided to detect a bifunctional molecule (named dBET1) induced PPI between cereblon and BRD4(1) (i.e., BRD4 bromodomain 1). dBET1 was designed by linking cereblon (CRBN)-binding IMiD and BRD4-binding ligand JQ1, and it was shown to induce BET protein degradation and delay leukemia progression in mice.[22] Using the Alphascreen assay, dBET1 was previously shown to induce the interaction between CRBN and BRD4(1). To design and demonstrate SPPIER for detecting dBET1-induced PPI in living cells, we genetically fused HO-Tag3 to CRBN and HO-Tag6 to BRD4(1). Coexpression of the two fusion proteins revealed homogeneous fluorescence in HEK293 cells (Figure 2A). Addition of dBET1 to the cells led to fast formation of EGFP droplets within a few minutes, indicated by the punctal green fluorescence. The intense brightness (10×) and simple signal pattern allowed straightforward and robust detection of the dBET1-induced interaction. Our data thus demonstrate that SPPIER enables robust detection of dBET1-induced PPI in living cells.

Next, we decided to show whether SPPIER can detect another bifunctional molecule (named ARV-825) induced PPI. ARV-825 was previously designed by chemically linking pomalidomide (a cereblon (CRBN)-binding IMiD) and OTX015 (a BRD4-binding ligand).[23] We coexpressed the two fusion proteins (CRBN-EGFP-HOTag3 and BRD4(1)-EGFP-HOTag6) in HEK293 cells. Addition of ARV-825 to the cells led to formation of EGFP droplets with intense brightness and simple signal pattern (Figure 2B), which indicates that SPPIER can detect ARV825-induced interaction between CRBN and BRD4(1).

We also examined whether SPPIER could be used to detect a bifunctional molecule (named ARV-771) induced PPI between the E3 ubiquitin ligase VHL (von Hippel−Lindau tumor suppressor protein) and BRD4(1).[24] ARV-771 was synthesized by linking a BET inhibitor and a VHL ligand, and it was shown to induce BET protein degradation and tumor regression in mice. To detect ARV771-induced PPI, we genetically fused HO-Tag3 and EGFP to VHL. Coexpression of VHL-EGFP-HOTag3 and BRD4(1)-EGFP-HOTag6 in HEK293 cells revealed homogeneous fluorescence in the absence of ARV-771, suggesting no interaction between VHL and BRD4(1) (Figure 2C). Addition of ARV-771 led to EGFP droplet formation (Figure 2C), indicating that ARV-771 did induce the PPI between VHL and BRD4(1). We also examined the specificity of SPPIER in detecting bifunctional molecule induced interaction. We added the three bifunctional molecules to cells expressing VHL-EGFP-HOTag3 and BRD4(1)-EGFP-HOTag6. While ARV-771 induced EGFP

DOI: 10.1021/acs.analchem.8b03476
Anal. Chem. 2018, 90, 14287−14293

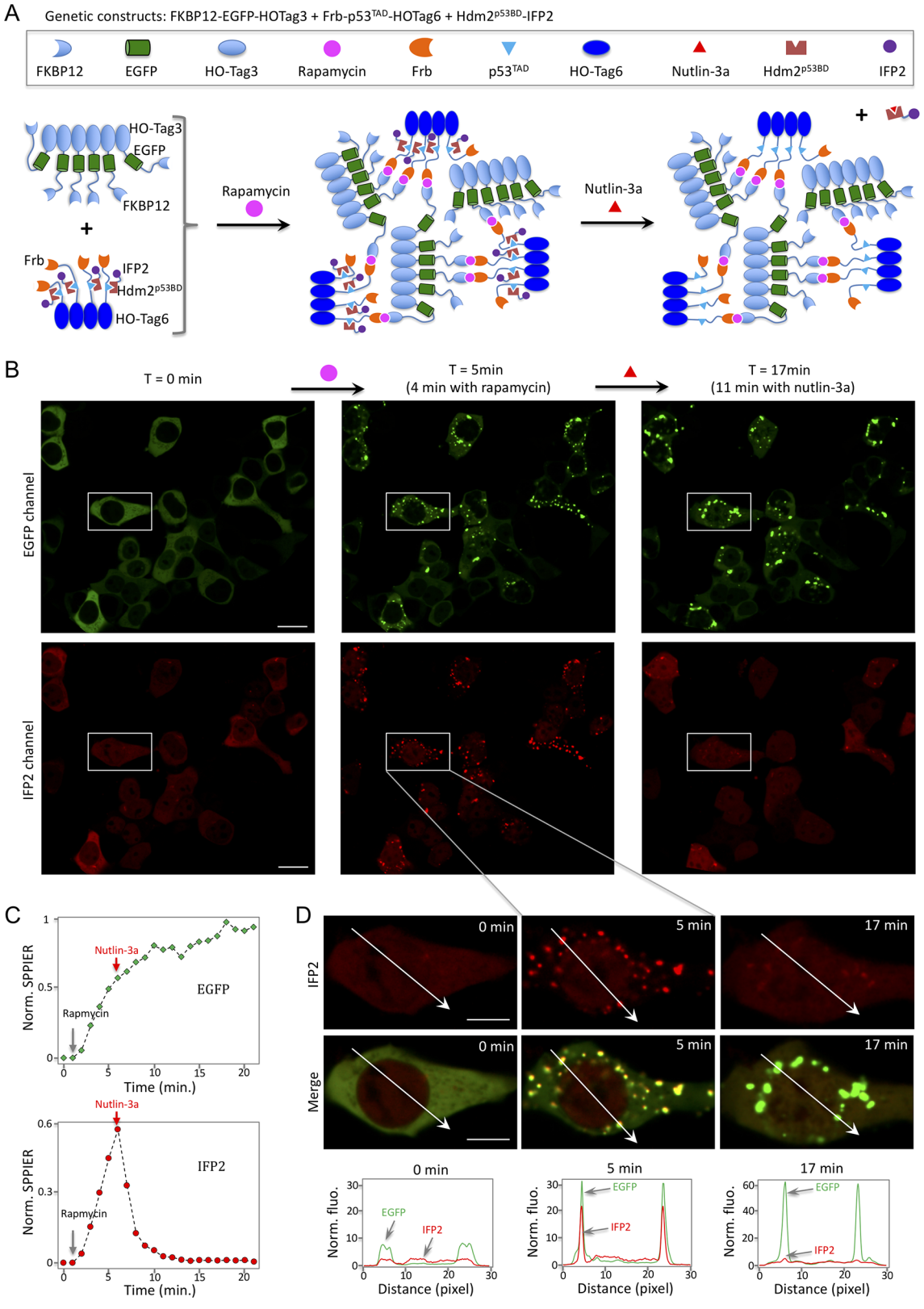

Figure 3. Inducible SPPIER detects small molecule induced dissociation of a protein complex in live cells. (A). Schematic of the design strategy for rapamycin-inducible SPPIER. (B). Time-lapse fluorescence images of HEK293 cells upon addition of rapamycin (0.1 μM), followed by nutlin-3a (10 μM). HEK293 cells transiently expressed FKBP12-EGFP-HOTag3, Frb-p53^{TAD}-HOTag6, and HDM2^{p53BD}-IFP2. IFP2 is an improved infrared fluorescent protein (IFP). (C). Kinetics of the green (top) and infrared (bottom) fluorescent SPPIER signal upon addition of rapamycin and nutlin-3a, corresponding to (B). (D). Time-lapse fluorescence images corresponding to the enlarged area shown in (B). A fluorescence histogram of the line across the cells is shown at the bottom. Scale bar: (B) 20 μm; (D) 10 μm.

DOI: 10.1021/acs.analchem.8b03476
Anal. Chem. 2018, 90, 14287−14293

droplet formation, the other two molecules did not (Figure 2D). Therefore, our data demonstrate that SPPIER can robustly and specifically detect bifunctional molecule induced PPIs in living cells.

SPPIER Is Reversible upon Removal of the PPI-Inducible Small Molecules. Finally, to demonstrate that SPPIER is reversible, i.e. the EGFP droplets are dependent on the small-molecule-induced PPI, we examined whether the EGFP droplets dissemble when ARV-825 is removed. We preincubated the cells with ARV-825 to induce EGFP phase separation and then washed the molecule and conducted time-lapse imaging. The punctal green fluorescence became homogeneous within 10 min, indicating that the EGFP droplets indeed dissembled quickly upon removal of the molecule (Figure 2E). As a control, without removal of ARV-825, the droplets were not disassembled over time and instead they coalesced into larger droplets (Video 3 in the Supporting Information). To quantify the data, we defined "SPPIER signal" as the sum of fluorescent droplet pixel intensity divided by the sum of cell pixel intensity. Analysis of the time-lapse imaging data indicated that the SPPIER signal decreased upon removal of the molecule, whereas the signal was stable over time when the small molecule was not washed (Figure 2E). Our data thus demonstrate that SPPIER can reversibly monitor small molecule induced PPIs in living cells. Additionally, we also applied SPPIER signals and quantified other time-lapse imaging data (Figure S2 in the Supporting Information). Furthermore, we showed that higher concentrations of ARV825 led to higher SPPIER signals (Figure S3 in the Supporting Information), indicating that SPPIER is dependent on the ligand concentration. Our data suggest that the EGFP droplets are formed via small molecule induced multivalent PPI.

Inducible SPPIER Visualizes Small Molecule Induced Protein−Protein Dissociation. After demonstration of SPPIER in detecting small molecule induced protein−protein association, we moved further to show if SPPIER can detect small molecule induced protein−protein dissociation. One of the well-established examples for small molecule based disruption of PPIs is nutlin-induced dissociation of HDM2 and p53.[6] p53 is a tumor suppressor and master regulator of diverse cellular processes.[25] It interacts with the E3 ligase HDM2, resulting in ubiquitination and degradation. HDM2 is often overexpressed in many human cancers. Nutlin-3a disrupts the interaction between p53 and HDM2 and thus stabilizes p53, leading to p53-dependent apoptosis.

To demonstrate SPPIER in nutlin-induced dissociation of HDM2/p53 complex, we designed an inducible SPPIER system (Figure 3A). In particular, we genetically fused HO-Tag6 to the transactivation domain (TAD) of p53 and Frb (Frb-p53^{TAD}-HOTag6), HO-Tag3 to EGFP and FKBP12 (FKBP12-EGFP-HOTag3), and IFP2 (an improved infrared fluorescent protein[26]) to the p53 binding domain (p53BD) of HDM2 (HDM2^{p53BD}-IFP2). Coexpression of these three fusion constructs in the HEK293 cells led to homogeneous green and infrared fluorescence (Figure 3B). Addition of rapamycin, which induces interaction between FKBP12 and Frb, resulted in rapid formation of green and infrared fluorescent droplets within a few minutes (Figure 3B−D, Videos 4 and 5 in the Supporting Information). Following this, we added nutlin-3a, which led to rapid disassembly of the infrared fluorescent droplets with a half-time of ∼2 min (Figure 3C). On the other hand, the green fluorescent droplets were not affected by nutlin-3a. These data demonstrate that SPPIER detects nutlin-3a-induced dissociation of p53 and HDM2. As a control, addition of DMSO instead of nutlin-3a did not disassemble infrared fluorescent droplets (Figure S4 in the Supporting Information).

CONCLUSIONS

We have developed a fluorophore phase transition-based PPI assay, SPPIER. It achieves large fluorescence change, high brightness, and fast and reversible kinetics in live cells. It robustly and specifically detects small molecule induced PPIs in living cells. We have further developed inducible SPPIER and demonstrated that it can detect small molecule induced dissociation of PPIs, suggesting that SPPIER may be used to screen for potent PPI inhibitors.

ASSOCIATED CONTENT

Supporting Information

The Supporting Information is available free of charge on the ACS Publications website at DOI: 10.1021/acs.analchem.8b03476.

Amino acid sequence of HO-Tag3 and HO-Tag6, Quantification of SPPIER signal related to time-lapse imaging data in Figures 1 and 2, SPPIER signal dependence on ligand concentration, and kinetics of the green and infrared) fluorescent SPPIER signal upon addition of rapamycin (0.1 μM) followed by DMSO (PDF)

Videos as described in the text (ZIP)

AUTHOR INFORMATION

Corresponding Author

*E-mail for X.S.: xiaokun.shu@ucsf.edu.

ORCID

Xiaokun Shu: 0000-0001-9248-7095

Notes

The authors declare the following competing financial interest(s): X.S. and C.-I.C. have filed a patent application covering this work.

ACKNOWLEDGMENTS

This work was supported by the NIH Director's New Innovator Award (1DP2GM105446).

REFERENCES

(1) Burslem, G. M.; Crews, C. M. *Chem. Rev.* **2017**, *117* (17), 11269−11301.

(2) Fischer, E. S.; Böhm, K.; Lydeard, J. R.; Yang, H.; Stadler, M. B.; Cavadini, S.; Nagel, J.; Serluca, F.; Acker, V.; Lingaraju, G. M.; Tichkule, R. B.; Schebesta, M.; Forrester, W. C.; Schirle, M.; Hassiepen, U.; Ottl, J.; Hild, M.; Beckwith, R. E. J.; Harper, J. W.; Jenkins, J. L.; Thomä, N. H. *Nature* **2014**, *512* (7512), 49−53.

(3) Krönke, J.; Udeshi, N. D.; Narla, A.; Grauman, P.; Hurst, S. N.; McConkey, M.; Svinkina, T.; Heckl, D.; Comer, E.; Li, X.; Ciarlo, C.; Hartman, E.; Munshi, N.; Schenone, M.; Schreiber, S. L.; Carr, S. A.; Ebert, B. L. *Science* **2014**, *343* (6168), 301−305.

(4) Lu, G.; Middleton, R. E.; Sun, H.; Naniong, M.; Ott, C. J.; Mitsiades, C. S.; Wong, K.-K.; Bradner, J. E.; Kaelin, W. G. *Science* **2014**, *343* (6168), 305−309.

(5) Ito, T.; Ando, H.; Suzuki, T.; Ogura, T.; Hotta, K.; Imamura, Y.; Yamaguchi, Y.; Handa, H. *Science* **2010**, *327* (5971), 1345−1350.

DOI: 10.1021/acs.analchem.8b03476
Anal. Chem. 2018, 90, 14287−14293

(6) Vassilev, L. T.; Vu, B. T.; Graves, B.; Carvajal, D.; Podlaski, F.; Filipovic, Z.; Kong, N.; Kammlott, U.; Lukacs, C.; Klein, C.; Fotouhi, N.; Liu, E. A. *Science* **2004**, *303* (5659), 844−848.
(7) Tsien, R. Y. *Angew. Chem., Int. Ed.* **2009**, *48* (31), 5612−5626.
(8) Tsien, R. Y. *Annu. Rev. Biochem.* **1998**, *67*, 509−544.
(9) Kerppola, T. K. *Annu. Rev. Biophys.* **2008**, *37* (1), 465−487.
(10) Kerppola, T. K. *Cold Spring Harbor Protocols* **2013**, *2013* (8). DOI: 10.1101/pdb.top076489
(11) Kiyokawa, E.; Aoki, K.; Nakamura, T.; Matsuda, M. *Annu. Rev. Pharmacol. Toxicol.* **2011**, *51* (1), 337−358.
(12) Ding, Y.; Li, J.; Enterina, J. R.; Shen, Y.; Zhang, I.; Tewson, P. H.; Mo, G. C. H.; Zhang, J.; Quinn, A. M.; Hughes, T. E.; Maysinger, D.; Alford, S. C.; Zhang, Y.; Campbell, R. E. *Nat. Methods* **2015**, *12* (3), 195−198.
(13) Alford, S. C.; Ding, Y.; Simmen, T.; Campbell, R. E. *ACS Synth. Biol.* **2012**, *1* (12), 569−575.
(14) Janzen, W. P. *Chem. Biol.* **2014**, *21* (9), 1162−1170.
(15) Zhang, Q.; Huang, H.; Zhang, L.; Wu, R.; Chung, C.-I.; Zhang, S.-Q.; Torra, J.; Schepis, A.; Coughlin, S. R.; Kornberg, T. B.; Shu, X. *Mol. Cell* **2018**, *69* (2), 334.
(16) Li, P.; Banjade, S.; Cheng, H.-C.; Kim, S.; Chen, B.; Guo, L.; Llaguno, M.; Hollingsworth, J. V.; King, D. S.; Banani, S. F.; Russo, P. S.; Jiang, Q.-X.; Nixon, B. T.; Rosen, M. K. *Nature* **2012**, *483* (7389), 336−340.
(17) Thomson, A. R.; Wood, C. W.; Burton, A. J.; Bartlett, G. J.; Sessions, R. B.; Brady, R. L.; Woolfson, D. N. *Science* **2014**, *346* (6208), 485−488.
(18) Grigoryan, G.; Kim, Y. H.; Acharya, R.; Axelrod, K.; Jain, R. M.; Willis, L.; Drndic, M.; Kikkawa, J. M.; DeGrado, W. F. *Science* **2011**, *332* (6033), 1071−1076.
(19) Watanabe, T.; Seki, T.; Fukano, T.; Sakaue-Sawano, A.; Karasawa, S.; Kubota, M.; Kurokawa, H.; Inoue, K.; Akatsuka, J.; Miyawaki, A. *Sci. Rep.* **2017**, *7*, 46380.
(20) Petzold, G.; Fischer, E. S.; Thomä, N. H. *Nature* **2016**, *532* (7597), 127−130.
(21) Matyskiela, M. E.; Ito, T.; Pagarigan, B.; Lu, C.-C.; Miller, K.; Fang, W.; Wang, N.-Y.; Nguyen, D.; Houston, J.; Carmel, G.; Tran, T.; Riley, M.; Nosaka, L.; Lander, G. C.; Gaidarova, S.; Xu, S.; Ruchelman, A. L.; Handa, H.; Carmichael, J.; Daniel, T. O.; Cathers, B. E.; Lopez-Girona, A.; Lu, G.; Chamberlain, P. P. *Nature* **2016**, *535* (7611), 252−257.
(22) Winter, G. E.; Buckley, D. L.; Paulk, J.; Roberts, J. M.; Souza, A.; Dhe-Paganon, S.; Bradner, J. E. *Science* **2015**, *348* (6241), 1376−1381.
(23) Lu, J.; Qian, Y.; Altieri, M.; Dong, H.; Wang, J.; Raina, K.; Hines, J.; Winkler, J. D.; Crew, A. P.; Coleman, K.; Crews, C. M. *Chem. Biol.* **2015**, *22* (6), 755−763.
(24) Raina, K.; Lu, J.; Qian, Y.; Altieri, M.; Gordon, D.; Rossi, A. M. K.; Wang, J.; Chen, X.; Dong, H.; Siu, K.; Winkler, J. D.; Crew, A. P.; Crews, C. M.; Coleman, K. G. *Proc. Natl. Acad. Sci. U. S. A.* **2016**, *113* (26), 7124−7129.
(25) Joerger, A. C.; Fersht, A. R. *Annu. Rev. Biochem.* **2016**, *85* (1), 375−404.
(26) Yu, D.; Gustafson, W. C.; Han, C.; Lafaye, C.; Noirclerc-Savoye, M.; Ge, W.-P.; Thayer, D. A.; Huang, H.; Kornberg, T. B.; Royant, A.; Jan, L. Y.; Jan, Y.-N.; Weiss, W. A.; Shu, X. *Nat. Commun.* **2014**, *5*, 3626.

DOI: 10.1021/acs.analchem.8b03476
Anal. Chem. 2018, 90, 14287−14293